NASA/CR—2005-213799

Capillary Driven Flows Along Differentially Wetted Interior Corners

C.L. Nardin and M.M. Weislogel
Portland State University, Portland, Oregon

June 2005

The NASA STI Program Office . . . in Profile

Since its founding, NASA has been dedicated to the advancement of aeronautics and space science. The NASA Scientific and Technical Information (STI) Program Office plays a key part in helping NASA maintain this important role.

The NASA STI Program Office is operated by Langley Research Center, the Lead Center for NASA's scientific and technical information. The NASA STI Program Office provides access to the NASA STI Database, the largest collection of aeronautical and space science STI in the world. The Program Office is also NASA's institutional mechanism for disseminating the results of its research and development activities. These results are published by NASA in the NASA STI Report Series, which includes the following report types:

- TECHNICAL PUBLICATION. Reports of completed research or a major significant phase of research that present the results of NASA programs and include extensive data or theoretical analysis. Includes compilations of significant scientific and technical data and information deemed to be of continuing reference value. NASA's counterpart of peer-reviewed formal professional papers but has less stringent limitations on manuscript length and extent of graphic presentations.

- TECHNICAL MEMORANDUM. Scientific and technical findings that are preliminary or of specialized interest, e.g., quick release reports, working papers, and bibliographies that contain minimal annotation. Does not contain extensive analysis.

- CONTRACTOR REPORT. Scientific and technical findings by NASA-sponsored contractors and grantees.

- CONFERENCE PUBLICATION. Collected papers from scientific and technical conferences, symposia, seminars, or other meetings sponsored or cosponsored by NASA.

- SPECIAL PUBLICATION. Scientific, technical, or historical information from NASA programs, projects, and missions, often concerned with subjects having substantial public interest.

- TECHNICAL TRANSLATION. English-language translations of foreign scientific and technical material pertinent to NASA's mission.

Specialized services that complement the STI Program Office's diverse offerings include creating custom thesauri, building customized databases, organizing and publishing research results . . . even providing videos.

For more information about the NASA STI Program Office, see the following:

- Access the NASA STI Program Home Page at ***http://www.sti.nasa.gov***

- E-mail your question via the Internet to help@sti.nasa.gov

- Fax your question to the NASA Access Help Desk at 301–621–0134

- Telephone the NASA Access Help Desk at 301–621–0390

- Write to:
  NASA Access Help Desk
  NASA Center for AeroSpace Information
  7121 Standard Drive
  Hanover, MD 21076

NASA/CR—2005-213799

Capillary Driven Flows Along Differentially Wetted Interior Corners

C.L. Nardin and M.M. Weislogel
Portland State University, Portland, Oregon

Prepared under Grant NAG3–2741

National Aeronautics and
Space Administration

Glenn Research Center

June 2005

Acknowledgments

The authors would like to thank colleague G. Recktenwald for helpful discussions concerning the numerical solutions. This work is supported in part by NASA's Microgravity Science and Applications Division through contract NAS3–00126 monitored by Enrique Ramé. C.L. Nardin is supported in part by the NASA Oregon Space Grant Consortium.

The authors credit Dieter Langbein's life (1932 - 2004), full of learning and teaching in the field of capillary phenomena condensed in his book, Capillary Surfaces: Shape - Stability - Dynamics, in Particular Under Weightlessness, Springer Tracts in Modern Physics, 178, Springer-Verlag 2002.

Available from

NASA Center for Aerospace Information
7121 Standard Drive
Hanover, MD 21076

National Technical Information Service
5285 Port Royal Road
Springfield, VA 22100

Available electronically at http://gltrs.grc.nasa.gov

Capillary Driven Flows Along Differentially Wetted Interior Corners

C.L. Nardin and M.M. Weislogel
Portland State University
Portland, Oregon 97207

Abstract

Closed-form analytic solutions useful for the design of capillary flows in a variety of containers possessing interior corners were recently collected and reviewed. Low-g drop tower and aircraft experiments performed at NASA to date show excellent agreement between theory and experiment for perfectly wetting fluids. The analytical expressions are general in terms of contact angle, but do not account for variations in contact angle between the various surfaces within the system. Such conditions may be desirable for capillary containment or to compute the behavior of capillary corner flows in containers consisting of different materials with widely varying wetting characteristics. A simple coordinate rotation is employed to recast the governing system of equations for flows in containers with interior corners with differing contact angles on the faces of the corner. The result is that a large number of capillary driven corner flows may be predicted with only slightly modified geometric functions dependent on corner angle and the two (or more) contact angles of the system. A numerical solution is employed to verify the new problem formulation. The benchmarked computations support the use of the existing theoretical approach to geometries with variable wetability. Simple experiments to confirm the theoretical findings are recommended. Favorable agreement between such experiments and the present theory may argue well for the extension of the analytic results to predict fluid performance in future large length scale capillary fluid systems for spacecraft as well as for small scale capillary systems on Earth.

Introduction

A variety of closed form solutions are available that predict important features of capillary driven flows along interior corners (ref. 1). Such flows are common in porous media and micro-fluidic devices, but are especially prevalent, and over large length scales, in the fluids management systems of spacecraft (ref. 2). For example, concerning the latter, interior corners are a common passive geometric solution to the positioning of liquid fuels and cryogens in their respective containers as shown in figure 1. In this figure the interior corners formed by vanes within a "spheriodal" tank (refs. 3 and 4) are shown to maintain the fuel over the outlet to the engine for proper operation during in-flight maneuvers in a low gravity environment.

Important characteristics of such flows include interface configurations, stability, and flow rate with respect to time and system perturbation. Solutions for flows in cylindrical polygonal geometries (refs. 5 to 8), planar and non-planar 'infinite' corners (refs. 9 to 11) and three-dimensional geometries (refs. 12 and 13) have been reported.

In this paper the generalized approach of previous analyses (ref. 8) is extended to capillary driven flows within planar interior corners where the wetting properties of the fluid differ between the two faces that form the interior corner. Such flows arise in systems consisting of differing materials, coatings, or other surface treatment. Several example problems are sketched in figure 2.

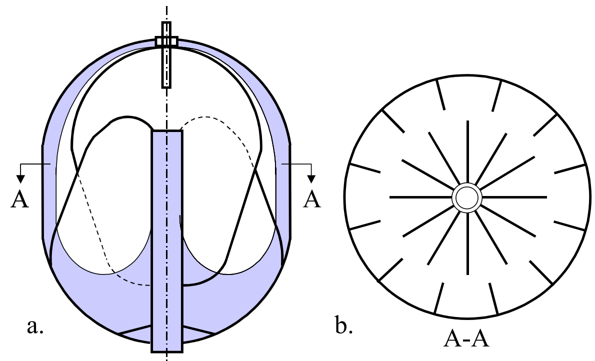

Figure 1.—Heavily vaned VTRE tank (refs. 3 and 4) schematic showing fluid location in low-g environment. Tank is partially liquid filled as shown in a. with fluid occupying shaded region.

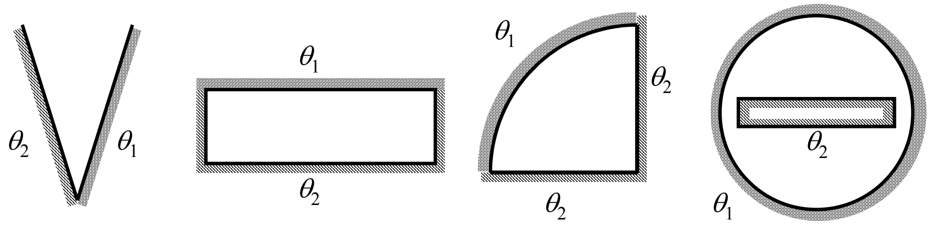

Figure 2.—Example container sections with variable wetabilities on various surfaces.

The differing wetabilities on each surface of the interior corner are characterized by contact angles θ_1 and θ_2. This work is pursued with the hope of providing simple geometrically dependent coefficients that can be used to modify the closed form solutions of previous investigators for a variety of problems as cited above.

Review of Problem Formulation

A schematic of a typical interior corner flow problem is sketched in figure 3 with characteristic dimensions noted for a system where $\theta_1 = \theta_2$. This is the case of previous investigations where the wetting characteristics are uniform between the fluid and walls of the corner producing a symmetric interface in the x–y-plane (fig. 3b).

In brief, by noting that the column of fluid in the corner is slender, namely $(H/L)^2 \equiv \varepsilon^2 \ll 1$, and that surface curvature ($\sim 1/Hf$) in the x–y-plane dominates the capillary pressure ($\varepsilon^2 f \ll 1$), where f is the measure of interface curvature, the free surface $S(y,z,t)$ may be expressed as a construct of circular arcs in x–y-planes that satisfy the slope condition (i.e., contact angle condition) at the wall. The Navier-Stokes equation reduces to the z-component equation only, which when integrated numerically can be used to determine the z-component velocity distribution $w(x,y,z,t)$. Numerically integrating this velocity over the cross-flow section (fig. 3b) yields the average velocity $\langle w \rangle = \langle w \rangle(z,t)$, which when substituted into the global mass balance equation in the z-direction yields a governing partial differential equation for a variety of flows differing only by respective boundary conditions. Proper scaling of the governing equations significantly reduces the reliance on numerical data.

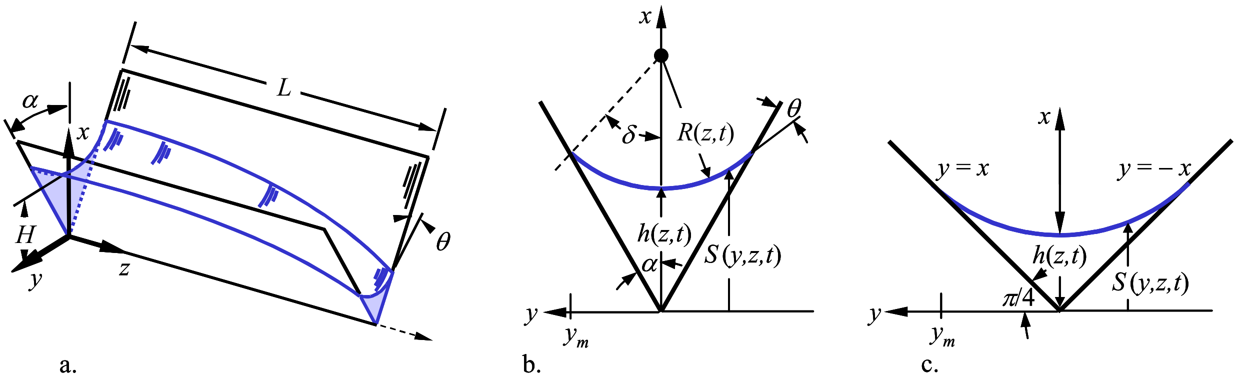

Figure 3.—Schematic of corner flow: a. characteristic dimensions, b. section detail, c. dimensionless section.

Choosing scales $x \sim H$, $y \sim H \tan\alpha$, $z \sim L$, $S \sim H$, $P \sim \sigma / Hf$, $t \sim L/W$, and

$$w \sim \frac{\varepsilon \sigma \sin^2 \alpha}{\mu f} \equiv W \,, \tag{1}$$

where

$$f = \frac{\sin\alpha}{\cos\theta - \sin\alpha} \,. \tag{2}$$

The dimensionless problem outlined above for $\varepsilon^2 \ll 1$ and $\varepsilon^2 f \ll 1$ yields free surface

$$S(y,h) = h(1+f) - (f^2 h^2 - y^2 \tan^2 \alpha)^{1/2} \,, \tag{3}$$

where $y \leq \left| f h \sin\delta / \tan\alpha \right|$, z-component momentum equation

$$P_z = w_{xx} \sin^2 \alpha + w_{yy} \cos^2 \alpha \tag{4}$$

subject to no slip on the walls

$$w = 0 \qquad \text{on} \qquad y = \pm x \,, \tag{5}$$

and no shear on the free surface

$$w_x - S_y w_y \cot^2 \alpha = 0 \qquad \text{on} \qquad x = S \,, \tag{6}$$

and the governing partial differential equation from global z-component mass balance, noting that $P_z = h_z / h^2$,

$$h_t = F_i\,(h_z^2 + h\,h_{zz})\,. \tag{7}$$

The dimensionless cross-flow problem, equations (4) to (6), is sketched in figure 3c. The dimensionless geometric flow resistance coefficient is $F_i = F_i\,(\theta,\alpha)$ must be determined numerically. However, due to the choice of scales for this problem, in particular W, $1/8 \lesssim F_i \leq 1/6$ for all values of θ and α satisfying the critical wetting condition studied mathematically by Concus and Finn (ref. 14), where $\theta < \pi/2 - \alpha$ in order to achieve the capillary flow condition studied here. For the remainder of this paper this condition shall be known as the C-F condition. If $\theta \geq \pi/2 - \alpha$ the liquid will not spread along the corner, but will retract until equilibrium is established. For many practical problems of interest F_i may be treated as a constant, say $F_i \approx 1/7$, and absorbed into the timescale of equation (7). The scale analysis method to determine W is presented in (ref. 10) and is instructive for subsequent equation nondimensionalization prior to asymptotic analyses. (The simple problem of fully developed laminar flow through a rectangular duct is revisited herein (Numerical Solution to Cross Flow Problem section) as a numerical benchmark and secondly to illustrate the utility of the general scaling approach. The hydraulic diameter and scale analysis solutions for average velocity are compared, the latter of which more narrowly brackets the exact solution for this problem.) The results of numerical solutions for $F_i\,(\alpha,\theta)$ also demonstrate the value of a correctly scaled geometry.

Formulation for Problem $\theta_1 \neq \theta_2$

A sketch of the dimensional corner flow cross-section for the two contact angle case is provided in figure 4a for a corner half-angle α. The corner is positioned symmetrically about the x'-axis, similarly as the corner in figure 3b. The C-F condition for this case is

$$\frac{\theta_1 + \theta_2}{2} < \frac{\pi}{2} - \alpha\ . \tag{8}$$

The further constraint of a partially wetting system, $\theta_1 \leq \pi/2$ and $\theta_2 \leq \pi/2$, places the interface behavior of interest here within the D_1^+-domain identified by Concus and Finn (ref. 15). The configuration of figure 4a is rotated in figure 4b such that the minimum height of the meniscus occurs along $y = 0$, which is to say that the radius of interface curvature in the x–y-plane pivots about a point on the x-axis whereas in figure 4a it does not. Thus, noting that $f_1 = f_2 = f$ and $\alpha_1 + \alpha_2 = 2\alpha$, α_1 and α_2 may be computed from

$$T_1 \equiv \tan\alpha_1 = \frac{\sin 2\alpha}{(N + \cos 2\alpha)} \tag{9}$$

and

$$T_2 \equiv \tan\alpha_2 = \frac{\sin 2\alpha}{N^{-1} + \cos 2\alpha}\,, \tag{10}$$

where

$$N = \frac{\cos\theta_2}{\cos\theta_1}. \tag{11}$$

To avoid redundancy in the analysis and computations to follow $\theta_1 \le \theta_2$ and $\alpha_1 \ge \alpha_2$ are defined. Thus, $0 \le N \le 1$ and $0 \le \theta_1/\theta_2 \le 1$. Note also that $\delta_1 = \pi/2 - \alpha_1 - \theta_1$ and $\delta_2 = \pi/2 - \alpha_2 - \theta_2$. By choosing alternative scales for y and w, namely; $y \sim TH$ and

$$w \sim W \equiv \frac{\varepsilon\sigma}{\mu f}\left(\frac{T^2}{1+T^2}\right), \tag{12}$$

where

$$T \equiv \frac{1}{2}\left(T_1 + T_2\right), \tag{13}$$

a convenient dimensionless cross flow problem is posed as sketched in figure 4c. In this figure the flow domain of figure 4b is stretched such that the dimensionless cross flow area is ~ $O(1)$ for all values of α, θ_1, and θ_2. The numeric problem of flow through the dimensional section sketched in figure 4b will be described shortly.

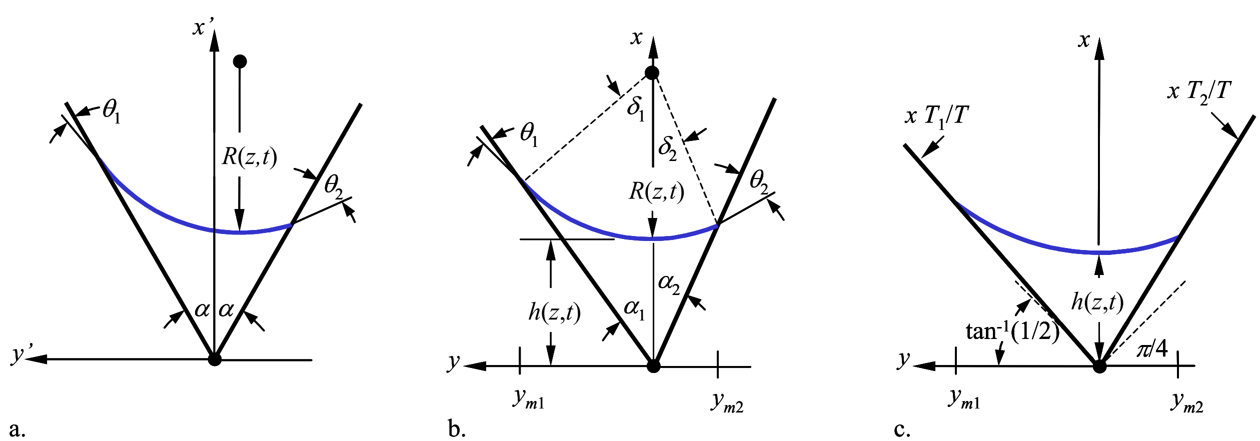

Figure 4.—Schematic representations of cross flow sections with differing wetabilities on faces of interior corner, θ_1, θ_2: a. Corner symmetric about dimensional x'-axis, b. Axes rotated such that radius of interface curvature aligns with dimensional x-axis, c. Dimensionless, rotated section.

The dimensionless geometric scaling function $T = T(\alpha,\theta_1,\theta_2)$ is used to account for the widely varying characteristic y-length scale arising for wide variations in α, θ_1, and θ_2. Some limiting cases for T are provided below:

1. Symmetry Condition, $\theta_1 = \theta_2$. For this condition $\alpha_1 = \alpha_2 = \alpha$ and $N = 1$. Thus, from equation (13),
2. $T = \tan \alpha$ and the governing system given by equations (1) to (7) is recovered.
3. Large Contact Angle, $\theta_2 \to \pi/2$ with $\alpha \le \pi/4$. For this condition, in order to satisfy the C-F condition (eq. (8)), $\theta_1 \ll 1$. Thus, $N \to 0$, $\alpha_2 \to 0$, and $\alpha_1 \to 2\alpha$, and from equation (13),
4. $T \to (1/2) \tan 2\alpha$.
5. Small Corner Limit, $\alpha \ll 1$. In this limit $T \sim \alpha$, which recovers the result of the symmetric scaling resulting in equation (4).
6. Large Corner Limit, $\alpha_2 \to \pi/2$. Defining $\Omega = \pi/2 - \alpha$, this limit is identical to $\Omega \ll 1$. Equation (13) reduces to $T \sim 1/\Omega$ when $\Omega \ll 1$, which also recovers the result of the symmetric scaling resulting in equations (4) to (6).

Thus, the limiting behavior of T for the $\theta_1 \neq \theta_2$ problem suggests that F_i computed numerically should be a narrowly bound function just as when computed using the symmetric scaling quantities for the $\theta_1 = \theta_2$ problem.

Modified System for Problem $\theta_1 \neq \theta_2$

The governing dimensionless system of equations again constrained by $\varepsilon^2 \ll 1$ and $\varepsilon^2 f \ll 1$ yields

$$f_1 \equiv \frac{\sin\alpha_1}{\cos\theta_1 - \sin\alpha_1} = f = \frac{\sin\alpha_2}{\cos\theta_2 - \sin\alpha_2} \equiv f_2, \tag{14}$$

free surface

$$S(y,h) = h(1+f) - (f^2h^2 - T^2y^2)^{1/2}, \tag{15}$$

where $\sin\delta_1 \le Ty/fh \le \sin\delta_2$, z-component momentum equation

$$P_z = \left(\frac{T^2}{1+T^2}\right) w_{xx} + \left(\frac{1}{1+T^2}\right) w_{yy}, \tag{16}$$

subject to no slip on the walls

$$w = 0 \qquad \text{on} \qquad y = \frac{x T_1}{T}, \tag{17}$$

$$w = 0 \qquad \text{on} \qquad y = -\frac{x T_2}{T}, \tag{18}$$

and no shear on the free surface

$$w_x - T^{-2} S_y w_y = 0 \qquad \text{on} \qquad x = S \ , \tag{19}$$

and again the governing partial differential equation from global z-component mass balance is equation (7).

Analytic Solutions to Cross-Flow Problem

The 'cross-flow' problem described by equations (16) to (19) may be solved analytically in the limits of large and small interior corner angle. Introducing $\Omega \equiv \pi/2 - \alpha$, these limits are described asymptotically by $\Omega^2 \ll 1$ and $\alpha^2 \ll 1$, respectively. Using normal series expansions of the dependent variables (w, P, and S) in powers of either Ω^2 or α^2, leading order expressions for F_i may be determined for comparisons with subsequent numerical calculations. Some important details of the asymptotic solution approach are provided here.

Large Corner Angle Solution, $\Omega^2 \ll 1$

The large angle limit is the condition $\alpha \to \pi/2$, or preferably $\Omega \to 0$. Choosing expansions

$$w = w_o + \Omega^2 w_1 + \ldots \tag{20}$$

$$P = P_o + \Omega^2 P_1 + \ldots \tag{21}$$

$$S = S_o + \Omega^2 S_1 + \ldots , \tag{22}$$

for conditions where $\Omega^2 \ll 1$, the governing z-component momentum equation (16) reduces to

$$P_z = w_{xx} + O(\Omega^2) . \tag{23}$$

The no slip boundary conditions on the walls, equations (17) and (18), remain unchanged, but the free surface shear stress condition equation (19) simplifies to

$$w_x = 0 + O(\Omega^2) \quad on \quad x = S_o \tag{24}$$

Because $P_z = h_z/h^2$ is not a function of x the velocity profile may be determined analytically from (23) producing

$$w_{o_1} = \frac{(1+T^2)\, h_z}{T^2 h^2} \left(\frac{x^2}{2} - \frac{T^2 y^2}{2 T_1^2} - S_o\, x + \frac{T\, S_o\, y}{T_1} \right) \equiv \frac{(1+T^2)\, h_z}{T^2 h^2} w_{o_1}^{+} \tag{25}$$

for $0 \le y \le y_{m1}$ and

$$w_{o_2} = \frac{(1+T^2)\,h_z}{T^2\,h^2}\left(\frac{x^2}{2} - \frac{T^2 y^2}{2T_2^2} - S_o\,x - \frac{T\,S_o\,y}{T_2}\right) \equiv \frac{(1+T^2)\,h_z}{T^2\,h^2}\,w_{o_2}^+ \tag{26}$$

for $y_{m2} \le y < 0$. The two flow regions are depicted in figure 4c. The average velocity over the cross-flow section may be determined by integrating equations (25) and (26) over their respective sections such that

$$\langle w_o \rangle = \frac{(1+T^2)\,h_z}{T\,h^4\,\overline{F}_A}\left[\int_0^{y_{m1}}\int_{Ty/T_1}^{S_o} w_{o_1}^+\;dx\,dy + \int_{y_{m2}}^{0}\int_{-Ty/T_2}^{S_o} w_{o_2}^+\;dx\,dy\right] \equiv -F_i\,h_z \tag{27}$$

where $y_{mi} = (-1)^{1+i}\,h\,f\sin(\Omega_i - \theta_i)/T$. The dimensionless area function $\overline{F}_A$ is given by

$$\overline{F}_A = (F_{A_1} + F_{A_2})/2\,, \tag{28}$$

where,

$$F_{A_i} = f^2\left(\frac{\cos\theta_i\,\sin(\Omega_i - \theta_i)}{\cos\Omega_i} - (\Omega_i - \theta_i)\right). \tag{29}$$

The analytic solution to equation (27) is simplified significantly by first writing each Ω_i and θ_i in terms of Ω and then expanding all geometric functions for small Ω. The following definitions are employed to this effect:

$$\Omega_1 = 2u\,\Omega/(1+u)\,,\ \Omega_2 = 2\,\Omega/(1+u)\,,\ \text{where } u \equiv \Omega_1/\Omega_2 \text{ with } \Omega_1 \le \Omega_2\,, \tag{30}$$

$$\theta_1^* \equiv (1+m)\,\theta_1/2\Omega\,,\ \theta_2^* \equiv (1+m)\,\theta_1/2\Omega\,,\ \text{where } m \equiv \theta_1/\theta_2\,,\ \theta_1 \le \theta_2\,, \tag{31}$$

and thus

$$\theta_1 = 2\,m\,\theta_2^*\,\Omega/(1+m)\,,\ \theta_2 = 2\,\theta_2^*\,\Omega/(1+m)\,. \tag{32}$$

Noting that $f = f_1 = f_2$, u may be determined analytically as a function of θ_2^* and m;

$$u = \frac{1-(1-m^2)\,\theta_2^*}{1+(1-m^2)\,\theta_2^*} + O(\Omega^2)\,. \tag{33}$$

With knowledge of u, equations (25) and (26) may be substituted into the terms present in equation (27) and the integration performed to reveal

$$F_i = \Big(5 + 20m_1\,\theta_2^* + 8\big(1 + 25\,m/2 + m^2\big)\theta_2^{*\,2} - 68\,m_1\big(1 - 50\,m/17 + m^2\big)\theta_2^{*\,3} - 70\,m_2^2\,(1+4m+m^2)\,\theta_2^{*\,4}$$

$$+140\, m_1\, m_2^4\, \theta_2^{*5} + 140\, m\, m_2^4\, \theta_2^{*6} - 28\, m_1\, m_2^6\, \theta_2^{*7} - 7\, m_1^2\, m_2^6\, \theta_2^{*8} \Big)$$

$$\div 35\left(1 - m_2^2 \theta_2^{*2}\right)^2 \left(1 + m_2 \theta_2^*\right)\left(1 + 2m_1\theta_2^* - 3m_2^2\theta_2^{*2}\right) + O(\Omega^2)\,, \tag{34}$$

where for brevity in this expression $m_1 \equiv 1+m$ and $m_2 \equiv 1-m$. Thus, under the constraint $\Omega^2 \ll 1$, $F_i = F_i(m, \theta_2^*)$. Some important limiting values of F_i are:

1. Symmetric wetting condition ($\theta_1 = \theta_2$): $m = 1$

$$F_i(1,\theta_2^*) = \frac{5 + 4(10 + 29\,\theta_2^* + 32\,\theta_2^{*2})\theta_2^*}{35\,(1 + 2\,\theta_2^*)^2\,(1 + 4\,\theta_2^*)} + O(\Omega^2)\,, \tag{35}$$

which agrees with previous analysis for this condition (ref. 16). Note that $F_i\,(1,0) = 1/7$.

2. The C-F condition ($\theta_1 + \theta_2 = 2\Omega$, or $\theta_1 + \theta_2 + 2\alpha = \pi$): $\theta_2^* = 1/(1+m)$

$$F_i = \frac{1}{6} + O(\Omega^2)\,. \tag{36}$$

For this flat interface configuration F_i is identical to the value determined analytically for the symmetrical problem for the C-F condition (ref. 16).

1. Perfect wetting ($\theta_1 = 0$): $m = 0$

$$F_i(0,\theta_2^*) = \frac{5 + 35\,\theta_2^* + 98\,\theta_2^{*2} + 126\,\theta_2^{*3} + 49\,\theta_2^{*4} + 7\,\theta_2^{*5}}{35\,(1 + \theta_2^*)^4\,(1 + 3\,\theta_2^*)} + O(\Omega^2) \tag{37}$$

For $\theta_2^* = 1$, $F_i(0,1) = 1/7$. Thus for all combinations of m and θ_2^*, $1/7 \le F_i(m, \theta_2^*) \le 1/6$ when $\Omega^2 \ll 1$.

Small Corner Angle Solution, $\alpha^2 \ll 1$

A similar asymptotic solution approach may be used to compute F_i for small corner angles where $\alpha^2 \ll 1$. Under these constraints equation (16) reduces to $P_z = w_{yy} + O(\alpha^2)$ and applying the appropriate boundary conditions leads to

$$w_o = \frac{(1+T^2)\,h_z}{2T^2\,h^2}\left(T_1\,T_2\,x^2 + T\,(T_1 - T_2)\,x\,y - T^2 y^2\right), \tag{38}$$

which applies for all y in the domain. Integration over the section yields

$$F_i = \frac{1}{6} + \alpha\, F(\theta_1, \theta_2) + O(\alpha^2) \tag{39}$$

where $F(\theta_1, \theta_2) \sim O(1)$ and is a known but cumbersome geometric quantity. It is sufficient here only to present the limiting values of F_i determined in this manner, and from equation (39), $F_i = 1/6 + O(\alpha)$for all values of θ_1 and θ_2.

Numerical Solution to Cross Flow Problem

The analytic results for F_i in the extreme limits of α, θ_1, and θ_2 offer compelling evidence that F_i is again a narrowly bounded function $\sim O(1/7) \le F_i \le 1/6$ for the $\theta_1 \ne \theta_2$ problem. However, for the majority of corner flows that do not appear to yield analytic solutions, equation (16) is solved numerically. The investigation is undertaken to verify the scaling employed for the $\theta_1 \ne \theta_2$ problem leading to the system of equations (14) through (19). If F_i can be confirmed to be bounded for all α, θ_1, and θ_2, similarly as for the case $\theta_1 = \theta_2$, then previous analytic solutions for a variety of problems can be resolved simply by replacing the flow resistance coefficient $F_i \sin^2 \alpha$ with $F_i\, T^2/(1 + T^2)$.

A Matlab® code written for this purpose is first benchmarked against the geometrically simpler problem of fully developed laminar flow in a rectangular duct for which an analytic solution is available for comparison. This problem serves to illustrate both the subtlety and importance of the non-dimensionalization for the numerical approach.

The system of equations (16) to (19) is then solved numerically and benchmarked against limiting values for the $\theta_1 = \theta_2$ problem that are analytic and/or have been computed by previous investigators (refs. 17 and 18). The term selected for comparison to the analytic results is the dimensionless flow resistance coefficient F_i which for the dimensionless problem provides proportionality between average z-component velocity and interface slope, or

$$\langle w \rangle = -F_i\, h_z\,. \tag{40}$$

[Note: The viscous resistance of the flow is actually inversely proportional to the nearly constant function F_i.] The numerically computed values for $\langle w \rangle$ are converted to F_i for the comparisons.

Benchmark: Fully Developed Laminar Duct Flow

The classic problem of single-phase (no interface) fully developed laminar flow through a rectangular duct of half width a and half height b is selected for use as a benchmark for the code. An exact solution to Poison's equation for this flow is available (ref. 19). The analytic equation for the dimensional average velocity is

$$\langle w \rangle_{exact} = -\frac{\Delta P\, a^2}{3\mu L}\left[1 - \frac{192}{\pi^5 \eta} \sum_{i=1,3,5,\ldots}^{\infty} \frac{\tanh(i\pi\eta/2)}{i^5}\right], \tag{41}$$

where, $\eta \equiv b/a$. Choosing length scales $x \sim a$, $y \sim b$ an identical scaling procedure as employed in the development of governing equations (14) and (16) produces the velocity scale,

$$w \sim W_{rect} \equiv \left(\frac{\Delta P}{\mu L}\right) \frac{b^2}{(1+\eta^2)}, \tag{42}$$

where, $P_z \equiv \Delta P / L$. Using this velocity scale, Poison's equation is nondimensionalized yielding the governing equation,

$$1 = \left(\frac{\eta^2}{1+\eta^2}\right) w_{xx} + \left(\frac{1}{1+\eta^2}\right) w_{yy} . \tag{43}$$

The modified Poison equation (43) for $w(x,y)$ is solved numerically and integrated over the domain to determine the nondimensional average velocity, which is redimensionalized for comparisons to the exact solution of equation (41). The computational error for representative values of η is displayed in figure 5. As observed from the figure, acceptable convergence is achieved when 50,000 or more elements are used. Contour plots for $\eta = 0$, $\eta = 1$, and $\eta \to \infty$ are presented in figure 6. The scaling permits accurate numerical solutions in the hard limits of $\eta = 0$ and $\eta \to \infty$. The value of the present scaling (W_{rect}, eq. (42)) is further illustrated by comparing to solutions obtained employing a hydraulic diameter scaling where $x \sim y \sim D_{hyd} \equiv ab/(a + b)$, defined such that limiting values of are equivalent for comparisons in figure 7),

$$W_{hyd} = \frac{\Delta P}{\mu L} \frac{b^2}{(1+\eta)^2} . \tag{44}$$

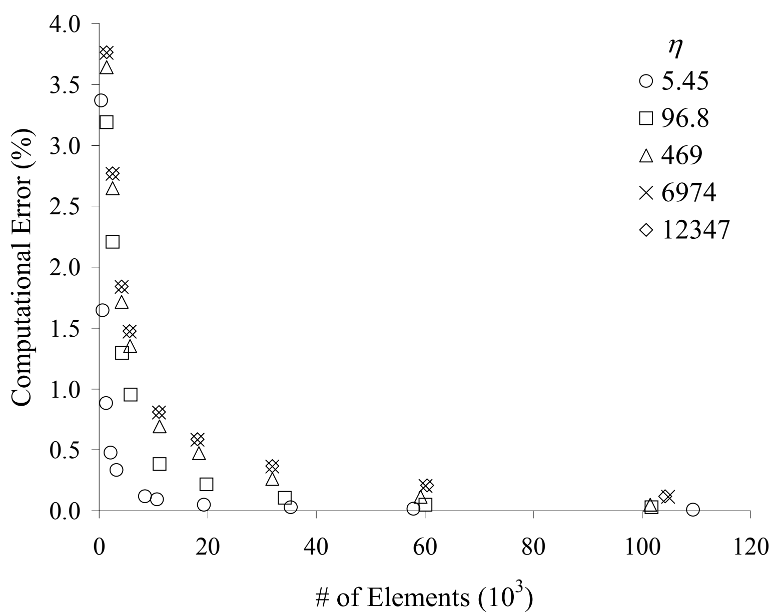

Figure 5.—Convergence study of fully developed laminar flow through a rectangular duct. The relative error calculation compares equation (41) to numerical solutions calculated with the Matlab® PDE Toolbox for various selections of η.

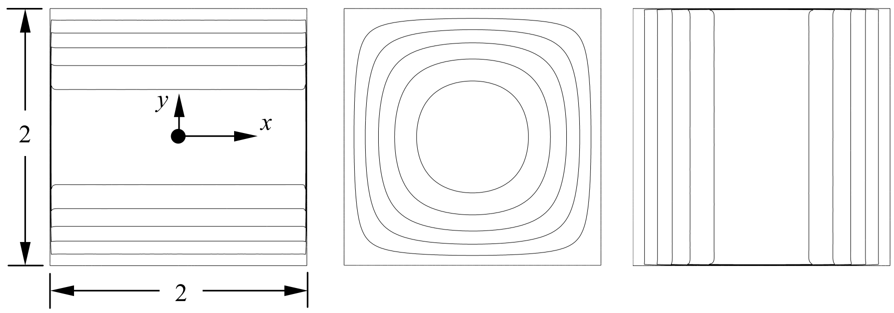

Figure 6.—Velocity contour maps in the scaled domain for rectangular duct flow. The left profile is for $\eta = 0$, the middle is $\eta = 1$, and the right is $\eta \to \infty$.

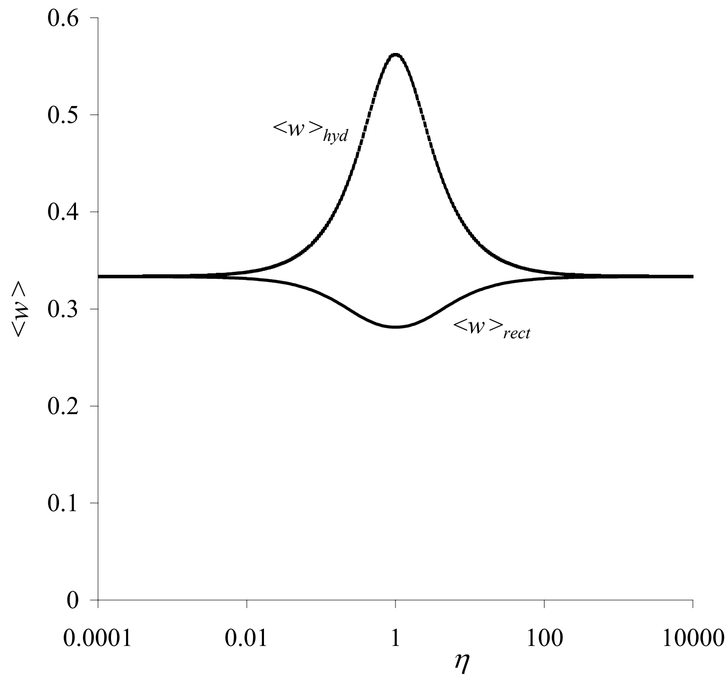

Figure 7.—Comparison of exact solution scaled by equation (42) and (44) respectively. The variation of $<w>$ for the former is significantly reduced.

The exact analytical solution for the average velocity through the rectangular duct equation (41) is normalized by both equation (42) and (44) scaling and presented in figure 7. The figure displays the extent to which the hydraulic diameter scaling increases the reliance on 'numerical data' over the full range of η, namely; $1/3 \leq \langle w \rangle_{hyd} \leq 9/16$, whereas $0.281\ldots \leq \langle w \rangle_{rect} \leq 1/3$. Thus, W_{rect} captures a higher degree of the flow's dependence on duct geometry and confines solutions for all η to a domain over 40 percent smaller than for the otherwise acceptable hydraulic diameter scaling. The scaling method for W, equation (12), for the corner flow problem addressed herein plays a similar role. [Note: Other methods to nondimensionalize this simple rectangular duct flow problem can lead to situations that are significantly worse than even the hydraulic diameter scaling. For example, Patzek and Silin (ref. 20) employ a dimensionless flow conductance $\widetilde{g}$ where $W_{PS} \sim \Delta P\, ab/\mu\, L$. When used to nondimensionalize equation (41), such a scaling does not produce results that are bounded by $O(1)$ constants, but rather $0 \leq \langle w \rangle \leq O(1)$ for all h, $0 \leq \eta \leq \infty$.]

Benchmark: Corner Flow with $\theta_1 = \theta_2$

The Matlab® numerical procedure is benchmarked for the corner flow problem for several analytic solutions of F_i with $\theta_1 = \theta_2 = \theta$. The favorable comparisons are shown in table 1. For case III, $\alpha = 89.8°$ is used to compute the numerical value of F_i; for all other cases the computations are carried out exactly as stated. As was the case for the rectangular duct, the fact that numerical data can be computed in the extreme limits of α and θ, is a result of the scaling of the problem, which produces ~ $O(1)$ area domains for all values of $0 \leq \alpha \leq \pi/2$, $0 \leq \theta_1 \leq \pi/2$ and $\theta_2 \leq \pi - 2\alpha - \theta_1$ satisfying the C-F condition.

When possible, and for the case $\theta_1 = \theta_2$, the numerical calculations are found to be in close agreement with the previous results of Ayyaswamy et al. (ref. 17) and Ransohoff and Radke (ref. 18).

Table 1.—Comparison of analytical and numerical values of F_i.

Case	Condition	Equation	F_i analytic	F_i numerical	Error (%)
I	$\alpha = 45°$ $\theta = 45°$	eq. (41) w/ $\eta = 1$	0.140577	0.140571	0.0044
II	$\alpha = 0$	eq. (39)	1/6	0.166664	0.0016
III	$\alpha \to 90°$ $\theta = 0$	eq. (35)	0.142857	0.142844	0.0091
IV	$\alpha = 90°$ $\delta = 0$	eq. (36)	1/6	0.166651	0.0094

Numerical Results for $F_i\,(\alpha,\theta_1,\theta_2)$

$F_i(\alpha,\theta_1,\theta_2)$ is determined numerically using Matlab® with PDE tool box in Microsoft Windows® on a 1 GHz machine with 512 Mb RAM. An adaptive mesh is employed containing a minimum of 50,000 elements and requiring 5 to 15 minutes to converge for a given choice of α, θ_1, θ_2. figure 8 presents over 2000 values of F_i computed for all wetting conditions satisfying the C-F condition and where $0 \leq \theta_1 \leq \theta_2 \leq \pi/2$ and $0 \leq \alpha \leq \pi/2$. It should be noted that certain wetting conditions have not been considered in this paper; specifically $\theta_2 > \pi/2$ with $\theta_1 < \pi - 2\alpha - \theta_2$. From figure 8 it is found that $1/9 \lesssim F_i \leq 1/6$ for all values chosen for α, θ_1 and θ_2. As observed in Table 1, the computational errors are extremely low, < 0.5 percent for these calculations. All computed values for $F_i(\alpha,\theta_1,\theta_2)$ are tabulated in the Appendix. For the problem $\theta_1 = \theta_2$, $1/8 \lesssim F_i \leq 1/6$. Thus, the scaling for the problem $\theta_1 \neq \theta_2$ problem, which recovers the results of problem $\theta_1 = \theta_2$ for symmetric wetting, yields a similar though slightly expanded range of values for F_i. Without a priori knowledge of the specific value of F_i one could assume $F_i \approx 1/7.2$ and be assured of at worst ±20 percent accuracy.

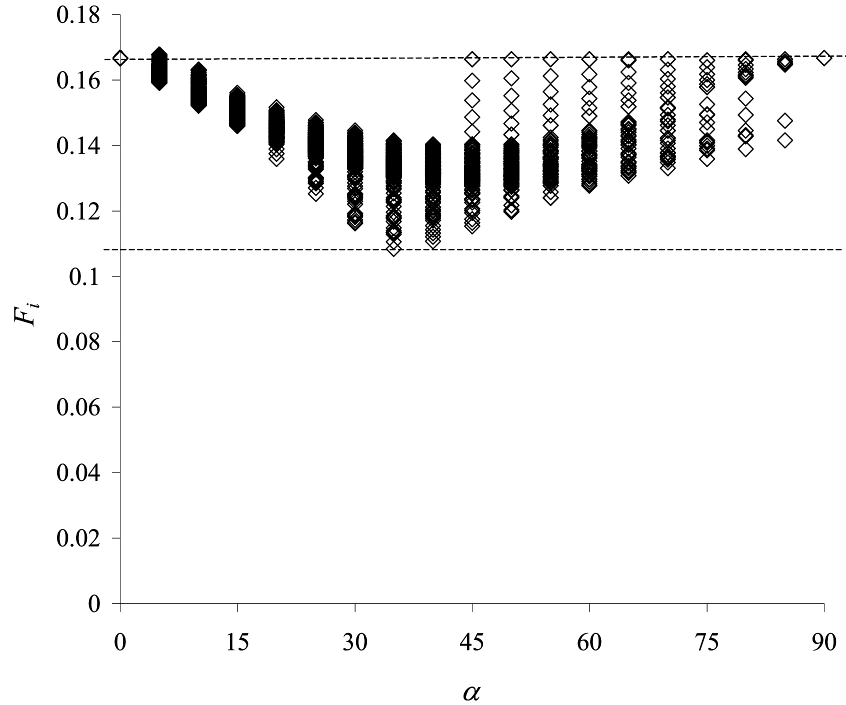

Figure 8.—Scatter plot showing all the numerically calculated values of $F_i(\alpha,\theta_1,\theta_2)$, where $(\theta_1 + \theta_2)/2 \le \pi/2 - \alpha$, $\theta_1 \le \pi/2$, $\theta_2 \le \pi/2$, and $0 \le \theta_1/\theta_2 \le 1$.

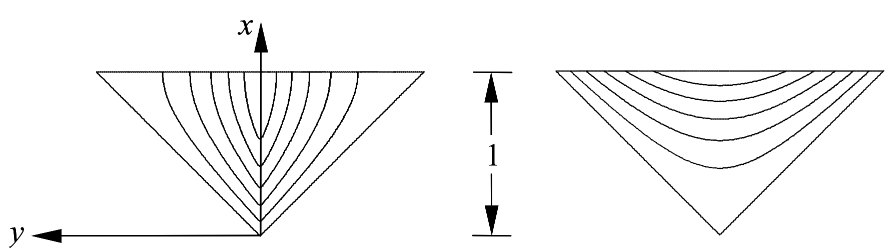

Figure 9.—Velocity contours in the scaled domain. The profile on the left is $\alpha = 0$ and on the right is $\alpha = \pi/2$.

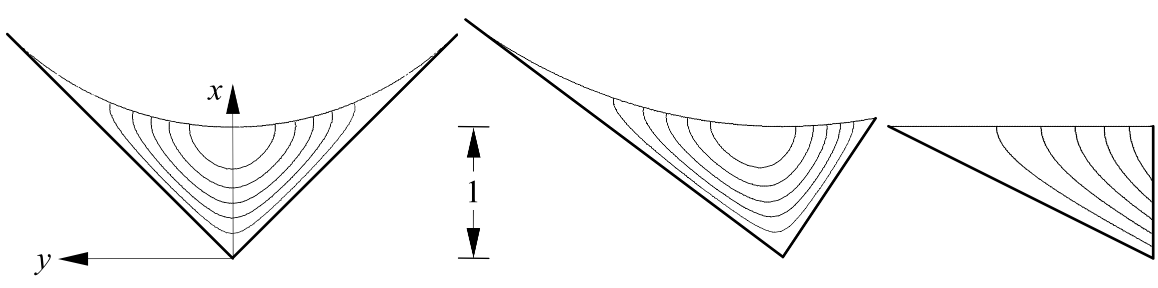

Figure 10.—Velocity contours in the scaled domain for $\alpha = \pi/4$. The profile on the left is for the wetting condition $\theta_1 = 0$ and $\theta_2 = 0$, the middle is $\theta_1 = 0$ and $\theta_2 = \pi/4$, and the right is $\theta_1 = 0$ and $\theta_2 = \pi/2$.

Application of Results

The recent review of corner flows (ref. 1) provides a collection of closed form solutions for a fixed contact angle ($\theta_1 = \theta_2$). The solutions are in part described by functions G and F_A which are modified by the results of this work for the two contact angle problem:

$$G = \frac{\sigma}{\mu}\frac{F_i \sin^2 \alpha}{f} \Rightarrow \frac{\sigma}{\mu}\frac{F_i}{f}\left(\frac{T^2}{1+T^2}\right) \tag{45}$$

$$F_A \Rightarrow \overline{F}_A \equiv \frac{1}{2}\left(F_{A1} + F_{A2}\right) \tag{46}$$

The dimensionless geometric viscous resistance function $T^2/(1 + T^2)$ for the general $\theta_1 \neq \theta_2$ replaces $\sin^2\alpha$ for the $\theta_1 = \theta_2$ problem. Recall that $T^2/(1 + T^2) = \sin^2\alpha$ when $\theta_1 = \theta_2$, since $T = (\tan\alpha_1 + \tan\alpha_2)/2$ with α_1 and α_2 given in equations (9) and (10). The dimensionless cross flow area function $\overline{F}_A$ represents the average of F_A values computed using θ_1 and θ_2. Note also that $\overline{F}_A = F_A$ when $\theta_1 = \theta_2$.
The more general forms for equations (45) and (46) may be simply substituted wherever they appear in (ref. 1) to determine the flow in corners for cases where $\theta_1 \neq \theta_2$.

From the values of F_i (α, θ_1, θ_2) listed in the Appendix it can be shown that errors in F_i of less than 5 percent are incurred using the simplifying approximation $F_i(\alpha, \theta_1, \theta_2) \approx F_i(\alpha, \theta_{ave})$ with $\theta_{ave} = (\theta_1 + \theta_2)/2$. The conditions under which this approximation holds are $\theta_2 - \theta_1 \lesssim \pi/6$ and/or $\alpha + \theta_2 \lesssim \pi/2$, where $0 \leq \theta_1 \leq \theta_2 \leq \pi/2$ and $0 \leq \alpha \leq \pi/2$.

The special case of spontaneous capillary rise requires the calculation of a constant height H boundary condition in each corner of the container where the C-F condition is satisfied. This may be accomplished by extending the method of de Lazzer et al. (ref. 21) to compute the radius of curvature of the interface R:

$$R = f_i H_i = \frac{\overline{P}}{2\Sigma}\left[1 - \left(1 - \frac{4A\Sigma}{\overline{P}^2}\right)^{1/2}\right], \tag{47}$$

where

$$\overline{P} = \sum_{i=1}^{n} P_i \cos\theta_i\ , \tag{48}$$

$$\Sigma = \sum_{i=1}^{n} \overline{F}_{An_i}\ , \tag{49}$$

$$\overline{F}_{An_i} = \overline{F}_{A_i} / f_i^2\ . \tag{50}$$

Σ is the total cross flow area function for the container and $\overline{P}$ is a section perimeter function weighted by $\cos\theta_i$ for each face of width P_i. A somewhat generalized polynomial container section for this flow scenario is represented schematically in figure 11 identifying the notation used in equation (47). When the C-F condition is not met in a particular corner i, $F_{Ani} = 0$ for that corner. Using this approach a global similarity solution for flows in all corners satisfying the C-F condition is also possible when $\theta_1 \neq \theta_2$ (refs. 4 and 7).

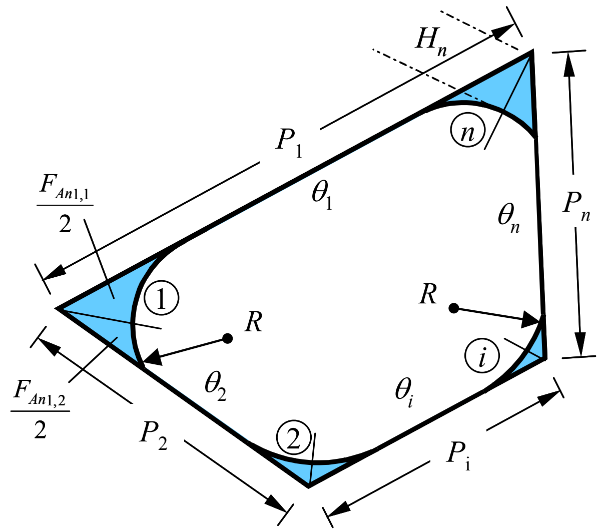

Figure 11.—*n*-sided polygonal section.

Recommended Experiments

Perhaps the simplest experiments capable of testing the theoretical work reported here are capillary rise drop tower experiments conducted in an identical manner as those performed by Weislogel and Lichter (ref. 8). In these experiments a right cylindrical container with interior corners is partially filled with a wetting liquid and place vertically in the drop tower test apparatus. Release of the experiment into free fall results in the spontaneous rise of liquid in the corners which is photographed at large working distances to accurately determine the interface location as a function of time.

The cross section of the container is critical to gather highly quantitative data from the images. For example, a right equilateral triangular cylindrical container can be constructed for the two contact angle condition with a priori knowledge of the contact angles of the two surfaces. A ray trace analysis can then be performed such that mismatched refractive indices between container and test fluid are minimized and the meniscus height $h(z,t)$ may be accurately imaged for comparison with predictions. In general, the containers should be designed such that the interface may be observed from the profile point of view of figure 4b rather than figure 4a. A sample sectional view of such a container is shown in figure 12.

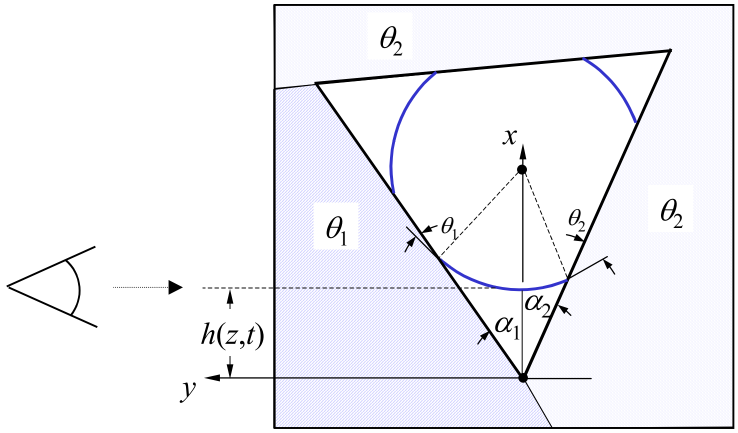

Figure 12.—Equilateral triangular container section with differing contact angles for drop tower tests. Line of sight shown at right (not to scale).

Concluding Remarks

The interior corner flow problem (for both $\theta_1 = \theta_2$ and $\theta_1 \neq \theta_2$) appears to be correctly scaled by the y length scale $y \sim TH$. This scaling produces a dimensionless flow resistance coefficient F_i that is calculated and computed herein and shown to be narrowly confined such that $1/9 \lesssim F_i \leq 1/6$. These results bode well for the many previous corner flow solutions that need only replace a coefficient to extend their relevance to flows where the wetting conditions on opposing faces of the corner differ.

References

1. Weislogel, M.M., Some Analytical Tools for Fluids Management in Space: Isothermal Capillary Flows Along Interior Corners, *Adv. Space Res*., **32**:2, pp. 163–170, (2003).
2. Jaekle, D.E. Jr., Propellant Management Device Conceptual Design and Analysis: Vanes, AIAA-SAE-ASME-ASEE 27th Jt. Propl. Conf., AIAA–91–2172, Sacramento, CA, (June 1991).
3. Chato, D.J., and Martin T.A., Vented Tank Resupply Experiment—flight test results, 33rd AIAA-ASME-SAE-ASEE Joint Propulsion Conference, AIAA–97–2815, July 6–9, Seattle, (1997).
4. Weislogel, M.M., and Collicott S.H., Analysis of Tank PMD Rewetting Following Thrust Resettling with a Post-Analysis of the Vented Tank Resupply Experiment, NASA/CR—2002-211974, (October, 2002).
5. Dong M., and Chatzis I., The Imbibition and Flow of a Wetting Liquid Along the Corners of a Square Capillary Tube, *J. Colloid and Int. Sci*., **172**, pp. 278–288 (1995).
6. Langbein, D., and Weislogel M.M., Dynamics of Liquids in Edges and Corners (DYLCO): IML-2 Experiment for the BDPU, NASA/TM—1998-207916 (1998).
7. Weislogel, M.M., Capillary Flow in Containers of Polygonal Section, *AIAA J*., **39**:12, pp. 2320–2326 (2001a).
8. Weislogel, M., Lichter, S., Capillary Flow in Interior Corners, *J. Fluid Mech*., **373**, pp. 349–378 (Nov. 1998).
9. Romero, L.A., and Yost, F.G., Flow in an Open Channel Capillary, *J. Fluid Mech*., **322**, pp. 109–129 (1996).

10. Weislogel, M.M., Capillary Flow in Interior Corners: the Infinite Column, *Phys. of Fluids*, **13**:11, pp. 3101–3107 (2001).
11. Weislogel, M.M., and Lichter, S., A Spreading Drop in an Interior Corner: Theory and Experiment, *Microgravity sci. technol*., **IX**:3, pp. 175–184 (1996).
12. Weislogel, M.M., Collicott, S.H., Capillary Re-Wetting of Vaned Containers: Spacecraft Tank Rewetting Following Thrust Resettling, *AIAA J*., vol. **42**, no. 12, pp. 2551–2607, Dec. 2004.
13. Weislogel, M.M., Steady Capillary Flow Along Interior Corners. (in preparation).
14. Concus, P, and Finn, R., On the Behavior of a Capillary Surface in a Wedge, *Proc. Acad. Sci*., **63**:2, pp. 292–299 (1969).
15. Concus, P., and Finn, R., Capillary Surfaces in a Wedge—Differing Contact Angles, *Microgravity sci. technol.,* **VII**:2, pp. 152-155 (1994).
16. Weislogel, M.M., Capillary Flow in an Interior Corner, NASA TM 107364 (1996).
17. Ayyaswamy, P.S., Catton, I., Edwards, D.K., Capillary Flow in Triangular Groves, ASME *J. of Applied Mech*., **41**, pp. 332-336 (1974).
18. Ransohoff, T.C., Radke, C.J., Laminar Flow of a Wetting Liquid along Corners of a Predominantly Gas-Occupied Noncircular Pore, *J. Colloid and Int. Sci*., **121**:2, p. 392 (Feb. 1988).
19. White, F., Viscous Fluid Flow, McGraw Hill, New York, Ch. 3 (1974).
20. Patzek, T.W. and Silin D.B., Shape Factor and Hydraulic Conductance in Noncircular Capillaries, *J. Colloid and Int. Sci*., **236**, pp. 295–304 (2001).
21. de Lazzer, A., Langbein, D., Dreyer, M., Rath, J., Mean Curvature of Liquid Surfaces in Containers of Arbitrary Cross-Section, *Microgravity Sci. Technol*., **IX**:3, pp. 208–219 (1996).

Appendix A—Tables 2 through 20
Computed Values of $F_i(\alpha,\theta_1,\theta_2)$.

The format for Tables 2 through 20 follows the form

α	θ_2	…
θ_1	$F_i(\alpha,\theta_1,\theta_2)$	…
…	…	…

Table 2.—$F_i(\alpha,\theta_1,\theta_2)$ for $\alpha = 0$.

0	0	5	10	15	20	25	30	35	40	45	50	55	60	65	70	75	80	85	90
0	0.167	0.167	0.167	0.167	0.167	0.167	0.167	0.167	0.167	0.167	0.167	0.167	0.167	0.167	0.167	0.167	0.167	0.167	0.167
5	0.167	0.167	0.167	0.167	0.167	0.167	0.167	0.167	0.167	0.167	0.167	0.167	0.167	0.167	0.167	0.167	0.167	0.167	0.167
10	0.167	0.167	0.167	0.167	0.167	0.167	0.167	0.167	0.167	0.167	0.167	0.167	0.167	0.167	0.167	0.167	0.167	0.167	0.167
15	0.167	0.167	0.167	0.167	0.167	0.167	0.167	0.167	0.167	0.167	0.167	0.167	0.167	0.167	0.167	0.167	0.167	0.167	0.167
20	0.167	0.167	0.167	0.167	0.167	0.167	0.167	0.167	0.167	0.167	0.167	0.167	0.167	0.167	0.167	0.167	0.167	0.167	0.167
25	0.167	0.167	0.167	0.167	0.167	0.167	0.167	0.167	0.167	0.167	0.167	0.167	0.167	0.167	0.167	0.167	0.167	0.167	0.167
30	0.167	0.167	0.167	0.167	0.167	0.167	0.167	0.167	0.167	0.167	0.167	0.167	0.167	0.167	0.167	0.167	0.167	0.167	0.167
35	0.167	0.167	0.167	0.167	0.167	0.167	0.167	0.167	0.167	0.167	0.167	0.167	0.167	0.167	0.167	0.167	0.167	0.167	0.167
40	0.167	0.167	0.167	0.167	0.167	0.167	0.167	0.167	0.167	0.167	0.167	0.167	0.167	0.167	0.167	0.167	0.167	0.167	0.167
45	0.167	0.167	0.167	0.167	0.167	0.167	0.167	0.167	0.167	0.167	0.167	0.167	0.167	0.167	0.167	0.167	0.167	0.167	0.167
50	0.167	0.167	0.167	0.167	0.167	0.167	0.167	0.167	0.167	0.167	0.167	0.167	0.167	0.167	0.167	0.167	0.167	0.167	0.167
55	0.167	0.167	0.167	0.167	0.167	0.167	0.167	0.167	0.167	0.167	0.167	0.167	0.167	0.167	0.167	0.167	0.167	0.167	0.167
60	0.167	0.167	0.167	0.167	0.167	0.167	0.167	0.167	0.167	0.167	0.167	0.167	0.167	0.167	0.167	0.167	0.167	0.167	0.167
65	0.167	0.167	0.167	0.167	0.167	0.167	0.167	0.167	0.167	0.167	0.167	0.167	0.167	0.167	0.167	0.167	0.167	0.167	0.167
70	0.167	0.167	0.167	0.167	0.167	0.167	0.167	0.167	0.167	0.167	0.167	0.167	0.167	0.167	0.167	0.167	0.167	0.167	0.167
75	0.167	0.167	0.167	0.167	0.167	0.167	0.167	0.167	0.167	0.167	0.167	0.167	0.167	0.167	0.167	0.167	0.167	0.167	0.167
80	0.167	0.167	0.167	0.167	0.167	0.167	0.167	0.167	0.167	0.167	0.167	0.167	0.167	0.167	0.167	0.167	0.167	0.167	0.167
85	0.167	0.167	0.167	0.167	0.167	0.167	0.167	0.167	0.167	0.167	0.167	0.167	0.167	0.167	0.167	0.167	0.167	0.167	0.167
90	0.167	0.167	0.167	0.167	0.167	0.167	0.167	0.167	0.167	0.167	0.167	0.167	0.167	0.167	0.167	0.167	0.167	0.167	0.167

Table 3.—$F_i(\alpha,\theta_1,\theta_2)$ for $\alpha = 5$.

5	0	5	10	15	20	25	30	35	40	45	50	55	60	65	70	75	80	85	90
0	0.159	0.159	0.159	0.159	0.159	0.160	0.160	0.160	0.160	0.160	0.161	0.161	0.162	0.162	0.163	0.164	0.165	0.166	0.168
5	0.159	0.159	0.159	0.159	0.159	0.160	0.160	0.160	0.160	0.160	0.161	0.161	0.162	0.162	0.163	0.164	0.165	0.166	0.168
10	0.159	0.159	0.159	0.159	0.160	0.160	0.160	0.160	0.160	0.160	0.161	0.161	0.162	0.162	0.163	0.164	0.165	0.166	0.168
15	0.159	0.159	0.159	0.159	0.160	0.160	0.160	0.160	0.160	0.160	0.161	0.161	0.162	0.162	0.163	0.164	0.165	0.166	0.168
20	0.159	0.159	0.160	0.160	0.160	0.160	0.160	0.160	0.160	0.161	0.161	0.161	0.162	0.162	0.163	0.164	0.165	0.166	0.168
25	0.160	0.160	0.160	0.160	0.160	0.160	0.160	0.160	0.160	0.161	0.161	0.161	0.162	0.162	0.163	0.164	0.165	0.166	0.168
30	0.160	0.160	0.160	0.160	0.160	0.160	0.160	0.160	0.161	0.161	0.161	0.161	0.162	0.162	0.163	0.164	0.165	0.166	0.167
35	0.160	0.160	0.160	0.160	0.160	0.160	0.160	0.160	0.161	0.161	0.161	0.161	0.162	0.162	0.163	0.164	0.165	0.166	0.167
40	0.160	0.160	0.160	0.160	0.160	0.160	0.161	0.161	0.161	0.161	0.161	0.161	0.162	0.162	0.163	0.163	0.164	0.165	0.167
45	0.160	0.160	0.160	0.160	0.161	0.161	0.161	0.161	0.161	0.161	0.161	0.161	0.162	0.162	0.163	0.163	0.164	0.165	0.166
50	0.161	0.161	0.161	0.161	0.161	0.161	0.161	0.161	0.161	0.161	0.161	0.162	0.162	0.162	0.163	0.163	0.164	0.165	0.166
55	0.161	0.161	0.161	0.161	0.161	0.161	0.161	0.161	0.161	0.161	0.162	0.162	0.162	0.162	0.163	0.163	0.164	0.165	0.166
60	0.162	0.162	0.162	0.162	0.162	0.162	0.162	0.162	0.162	0.162	0.162	0.162	0.162	0.162	0.163	0.163	0.164	0.164	0.165
65	0.162	0.162	0.162	0.162	0.162	0.162	0.162	0.162	0.162	0.162	0.162	0.162	0.162	0.163	0.163	0.163	0.164	0.164	0.165
70	0.163	0.163	0.163	0.163	0.163	0.163	0.163	0.163	0.163	0.163	0.163	0.163	0.163	0.163	0.163	0.163	0.164	0.164	0.164
75	0.164	0.164	0.164	0.164	0.164	0.164	0.164	0.164	0.163	0.163	0.163	0.163	0.163	0.163	0.163	0.164	0.164	0.164	0.164
80	0.165	0.165	0.165	0.165	0.165	0.165	0.165	0.165	0.164	0.164	0.164	0.164	0.164	0.164	0.164	0.164	0.164	0.164	0.164
85	0.166	0.166	0.166	0.166	0.166	0.166	0.166	0.166	0.165	0.165	0.165	0.165	0.164	0.164	0.164	0.164	0.164	0.165	
90	0.168	0.168	0.168	0.168	0.168	0.168	0.167	0.167	0.167	0.166	0.166	0.166	0.165	0.165	0.164	0.164	0.164		

Table 4.—$F_i(\alpha,\theta_1,\theta_2)$ for $\alpha = 10$.

10	0	5	10	15	20	25	30	35	40	45	50	55	60	65	70	75	80	85	90
0	0.152	0.152	0.152	0.153	0.153	0.153	0.153	0.153	0.154	0.154	0.155	0.155	0.156	0.157	0.158	0.159	0.160	0.161	0.163
5	0.152	0.152	0.152	0.153	0.153	0.153	0.153	0.153	0.154	0.154	0.155	0.155	0.156	0.157	0.158	0.159	0.160	0.161	0.163
10	0.152	0.152	0.153	0.153	0.153	0.153	0.153	0.154	0.154	0.154	0.155	0.155	0.156	0.157	0.158	0.159	0.160	0.162	0.163
15	0.153	0.153	0.153	0.153	0.153	0.153	0.153	0.154	0.154	0.154	0.155	0.155	0.156	0.157	0.158	0.159	0.160	0.162	0.163
20	0.153	0.153	0.153	0.153	0.153	0.153	0.154	0.154	0.154	0.155	0.155	0.156	0.156	0.157	0.158	0.159	0.160	0.162	0.163
25	0.153	0.153	0.153	0.153	0.153	0.154	0.154	0.154	0.154	0.155	0.155	0.156	0.156	0.157	0.158	0.159	0.160	0.162	0.163
30	0.153	0.153	0.153	0.153	0.154	0.154	0.154	0.154	0.155	0.155	0.155	0.156	0.156	0.157	0.158	0.159	0.160	0.161	0.162
35	0.153	0.153	0.154	0.154	0.154	0.154	0.154	0.155	0.155	0.155	0.156	0.156	0.157	0.157	0.158	0.159	0.160	0.161	0.162
40	0.154	0.154	0.154	0.154	0.154	0.154	0.155	0.155	0.155	0.155	0.156	0.156	0.156	0.157	0.157	0.158	0.159	0.160	0.161	0.161
45	0.154	0.154	0.154	0.154	0.155	0.155	0.155	0.155	0.155	0.156	0.156	0.156	0.157	0.157	0.158	0.159	0.159	0.160	0.160
50	0.155	0.155	0.155	0.155	0.155	0.155	0.155	0.156	0.156	0.156	0.156	0.156	0.157	0.157	0.158	0.159	0.159	0.160	0.160
55	0.155	0.155	0.155	0.155	0.156	0.156	0.156	0.156	0.156	0.156	0.156	0.157	0.157	0.158	0.158	0.159	0.159	0.159	0.159
60	0.156	0.156	0.156	0.156	0.156	0.156	0.156	0.157	0.157	0.157	0.157	0.157	0.157	0.158	0.158	0.159	0.159	0.159	0.158
65	0.157	0.157	0.157	0.157	0.157	0.157	0.157	0.157	0.157	0.157	0.157	0.158	0.158	0.158	0.159	0.159	0.159	0.159	0.157
70	0.158	0.158	0.158	0.158	0.158	0.158	0.158	0.158	0.158	0.158	0.158	0.158	0.158	0.159	0.159	0.159	0.160	0.159	0.156
75	0.159	0.159	0.159	0.159	0.159	0.159	0.159	0.159	0.159	0.159	0.159	0.159	0.159	0.159	0.159	0.160	0.160	0.160	
80	0.160	0.160	0.160	0.160	0.160	0.160	0.160	0.160	0.160	0.159	0.159	0.159	0.159	0.159	0.160	0.160	0.161		
85	0.161	0.161	0.162	0.162	0.162	0.162	0.161	0.161	0.161	0.160	0.160	0.159	0.159	0.159	0.159	0.160			
90	0.163	0.163	0.163	0.163	0.163	0.163	0.162	0.162	0.161	0.160	0.160	0.159	0.158	0.157	0.156				

Table 5.—$F_i(\alpha,\theta_1,\theta_2)$ for $\alpha = 15$.

15	0	5	10	15	20	25	30	35	40	45	50	55	60	65	70	75	80	85	90
0	0.146	0.146	0.146	0.146	0.147	0.147	0.147	0.148	0.148	0.149	0.149	0.150	0.150	0.151	0.152	0.153	0.153	0.154	0.154
5	0.146	0.146	0.146	0.147	0.147	0.147	0.147	0.148	0.148	0.149	0.149	0.150	0.150	0.151	0.152	0.153	0.153	0.154	0.154
10	0.146	0.146	0.146	0.147	0.147	0.147	0.148	0.148	0.148	0.149	0.149	0.150	0.151	0.151	0.152	0.153	0.154	0.154	0.154
15	0.146	0.147	0.147	0.147	0.147	0.148	0.148	0.148	0.149	0.149	0.150	0.150	0.151	0.152	0.152	0.153	0.154	0.154	0.154
20	0.147	0.147	0.147	0.147	0.147	0.148	0.148	0.148	0.149	0.149	0.150	0.150	0.151	0.152	0.153	0.153	0.154	0.154	0.154
25	0.147	0.147	0.147	0.148	0.148	0.148	0.148	0.149	0.149	0.150	0.150	0.151	0.151	0.152	0.153	0.153	0.154	0.154	0.154
30	0.147	0.147	0.148	0.148	0.148	0.148	0.149	0.149	0.149	0.150	0.150	0.151	0.151	0.152	0.153	0.153	0.154	0.154	0.153
35	0.148	0.148	0.148	0.148	0.148	0.149	0.149	0.149	0.150	0.150	0.151	0.151	0.152	0.152	0.153	0.153	0.154	0.154	0.152
40	0.148	0.148	0.148	0.149	0.149	0.149	0.149	0.150	0.150	0.150	0.151	0.151	0.152	0.152	0.153	0.153	0.154	0.153	0.151
45	0.149	0.149	0.149	0.149	0.149	0.150	0.150	0.150	0.150	0.151	0.151	0.152	0.152	0.153	0.153	0.153	0.153	0.153	0.150
50	0.149	0.149	0.149	0.150	0.150	0.150	0.150	0.151	0.151	0.151	0.151	0.152	0.152	0.153	0.153	0.153	0.153	0.152	0.149
55	0.150	0.150	0.150	0.150	0.150	0.151	0.151	0.151	0.151	0.152	0.152	0.152	0.153	0.153	0.154	0.154	0.153	0.152	0.148
60	0.150	0.150	0.151	0.151	0.151	0.151	0.151	0.152	0.152	0.152	0.152	0.153	0.153	0.154	0.154	0.154	0.154	0.152	0.147
65	0.151	0.151	0.151	0.152	0.152	0.152	0.152	0.152	0.152	0.153	0.153	0.153	0.154	0.154	0.154	0.155	0.154	0.152	
70	0.152	0.152	0.152	0.152	0.153	0.153	0.153	0.153	0.153	0.153	0.153	0.154	0.154	0.154	0.155	0.155	0.155		
75	0.153	0.153	0.153	0.153	0.153	0.153	0.153	0.153	0.153	0.153	0.153	0.154	0.154	0.155	0.155	0.156			
80	0.153	0.153	0.154	0.154	0.154	0.154	0.154	0.154	0.154	0.153	0.153	0.153	0.154	0.154	0.155				
85	0.154	0.154	0.154	0.154	0.154	0.154	0.154	0.154	0.153	0.153	0.152	0.152	0.152	0.152					
90	0.154	0.154	0.154	0.154	0.154	0.154	0.153	0.152	0.151	0.150	0.149	0.148	0.147						

Table 6.—$F_i(\alpha,\theta_1,\theta_2)$ for $\alpha = 20$.

20	0	5	10	15	20	25	30	35	40	45	50	55	60	65	70	75	80	85	90
0	0.141	0.141	0.141	0.141	0.142	0.142	0.142	0.143	0.143	0.144	0.144	0.144	0.145	0.145	0.146	0.146	0.145	0.144	0.142
5	0.141	0.141	0.141	0.141	0.142	0.142	0.142	0.143	0.143	0.144	0.144	0.145	0.145	0.145	0.146	0.146	0.145	0.144	0.142
10	0.141	0.141	0.141	0.142	0.142	0.142	0.143	0.143	0.144	0.144	0.144	0.145	0.145	0.146	0.146	0.146	0.146	0.145	0.143
15	0.141	0.141	0.142	0.142	0.142	0.143	0.143	0.143	0.144	0.144	0.145	0.145	0.146	0.146	0.147	0.147	0.146	0.145	0.143
20	0.142	0.142	0.142	0.142	0.143	0.143	0.143	0.144	0.144	0.145	0.145	0.146	0.146	0.147	0.147	0.147	0.146	0.145	0.143
25	0.142	0.142	0.142	0.143	0.143	0.143	0.144	0.144	0.145	0.145	0.146	0.146	0.147	0.147	0.147	0.147	0.147	0.145	0.142
30	0.142	0.142	0.143	0.143	0.143	0.144	0.144	0.145	0.145	0.145	0.146	0.146	0.147	0.147	0.148	0.147	0.147	0.145	0.141
35	0.143	0.143	0.143	0.143	0.144	0.144	0.145	0.145	0.145	0.146	0.146	0.147	0.147	0.148	0.148	0.147	0.146	0.144	0.140
40	0.143	0.143	0.144	0.144	0.144	0.145	0.145	0.145	0.146	0.146	0.147	0.147	0.148	0.148	0.148	0.148	0.146	0.144	0.139
45	0.144	0.144	0.144	0.144	0.145	0.145	0.145	0.146	0.146	0.147	0.147	0.148	0.148	0.148	0.148	0.148	0.146	0.143	0.137
50	0.144	0.144	0.144	0.145	0.145	0.146	0.146	0.146	0.147	0.147	0.148	0.148	0.148	0.149	0.149	0.148	0.146	0.143	0.136
55	0.144	0.145	0.145	0.145	0.146	0.146	0.146	0.147	0.147	0.148	0.148	0.148	0.149	0.149	0.149	0.149	0.147	0.142	
60	0.145	0.145	0.145	0.146	0.146	0.147	0.147	0.147	0.148	0.148	0.148	0.149	0.149	0.150	0.150	0.149	0.147		
65	0.145	0.145	0.146	0.146	0.147	0.147	0.147	0.148	0.148	0.148	0.149	0.149	0.150	0.150	0.151	0.151			
70	0.146	0.146	0.146	0.147	0.147	0.147	0.148	0.148	0.148	0.148	0.149	0.149	0.150	0.151	0.152				
75	0.146	0.146	0.146	0.147	0.147	0.147	0.147	0.147	0.148	0.148	0.148	0.149	0.149	0.151					
80	0.145	0.145	0.146	0.146	0.146	0.147	0.147	0.146	0.146	0.146	0.146	0.147	0.147						
85	0.144	0.144	0.145	0.145	0.145	0.145	0.145	0.144	0.144	0.143	0.143	0.142							
90	0.142	0.142	0.143	0.143	0.143	0.142	0.141	0.140	0.139	0.137	0.136								

Table 7.—$F_i(\alpha,\theta_1,\theta_2)$ for $\alpha = 25$.

25	0	5	10	15	20	25	30	35	40	45	50	55	60	65	70	75	80	85	90
0	0.136	0.137	0.137	0.137	0.138	0.138	0.138	0.139	0.139	0.139	0.140	0.140	0.140	0.140	0.139	0.138	0.136	0.133	0.129
5	0.137	0.137	0.137	0.137	0.138	0.138	0.138	0.139	0.139	0.140	0.140	0.140	0.140	0.140	0.140	0.138	0.137	0.134	0.129
10	0.137	0.137	0.137	0.138	0.138	0.138	0.139	0.139	0.140	0.140	0.140	0.141	0.141	0.141	0.140	0.139	0.137	0.134	0.130
15	0.137	0.137	0.138	0.138	0.138	0.139	0.139	0.140	0.140	0.141	0.141	0.141	0.141	0.141	0.141	0.140	0.138	0.135	0.130
20	0.138	0.138	0.138	0.138	0.139	0.139	0.140	0.140	0.141	0.141	0.141	0.142	0.142	0.142	0.141	0.140	0.138	0.135	0.130
25	0.138	0.138	0.138	0.139	0.139	0.140	0.140	0.141	0.141	0.142	0.142	0.142	0.142	0.142	0.142	0.141	0.139	0.135	0.129
30	0.138	0.138	0.139	0.139	0.140	0.140	0.141	0.141	0.142	0.142	0.142	0.143	0.143	0.143	0.142	0.141	0.139	0.135	0.128
35	0.139	0.139	0.139	0.140	0.140	0.141	0.141	0.142	0.142	0.143	0.143	0.143	0.144	0.143	0.143	0.141	0.139	0.134	0.127
40	0.139	0.139	0.140	0.140	0.141	0.141	0.142	0.142	0.143	0.143	0.143	0.144	0.144	0.144	0.143	0.142	0.139	0.133	0.125
45	0.139	0.140	0.140	0.141	0.141	0.142	0.142	0.143	0.143	0.144	0.144	0.144	0.145	0.145	0.144	0.142	0.139	0.133	
50	0.140	0.140	0.140	0.141	0.141	0.142	0.142	0.143	0.143	0.144	0.144	0.145	0.145	0.145	0.145	0.143	0.139		
55	0.140	0.140	0.141	0.141	0.142	0.142	0.143	0.143	0.144	0.144	0.145	0.146	0.146	0.146	0.146	0.144			
60	0.140	0.140	0.141	0.141	0.142	0.142	0.143	0.144	0.144	0.145	0.145	0.146	0.147	0.147	0.147				
65	0.140	0.140	0.141	0.141	0.142	0.142	0.143	0.143	0.144	0.145	0.145	0.146	0.147	0.148					
70	0.139	0.140	0.140	0.141	0.141	0.142	0.142	0.143	0.143	0.144	0.145	0.146	0.147						
75	0.138	0.138	0.139	0.140	0.140	0.141	0.141	0.141	0.142	0.142	0.143	0.144							
80	0.136	0.137	0.137	0.138	0.138	0.139	0.139	0.139	0.139	0.139	0.139								
85	0.133	0.134	0.134	0.135	0.135	0.135	0.135	0.134	0.133	0.133									
90	0.129	0.129	0.130	0.130	0.130	0.129	0.128	0.127	0.125										

Table 8.—$F_i(\alpha,\theta_1,\theta_2)$ for $\alpha = 30$.

30	0	5	10	15	20	25	30	35	40	45	50	55	60	65	70	75	80	85	90
0	0.133	0.133	0.133	0.134	0.134	0.135	0.135	0.136	0.136	0.136	0.136	0.136	0.135	0.134	0.133	0.130	0.127	0.122	0.116
5	0.133	0.133	0.134	0.134	0.135	0.135	0.135	0.136	0.136	0.136	0.136	0.136	0.136	0.135	0.133	0.131	0.128	0.123	0.117
10	0.133	0.134	0.134	0.134	0.135	0.135	0.136	0.136	0.136	0.137	0.137	0.137	0.137	0.136	0.134	0.132	0.129	0.124	0.118
15	0.134	0.134	0.134	0.135	0.135	0.136	0.136	0.137	0.137	0.138	0.138	0.138	0.137	0.137	0.135	0.133	0.130	0.125	0.119
20	0.134	0.135	0.135	0.135	0.136	0.137	0.137	0.137	0.138	0.138	0.138	0.138	0.138	0.138	0.136	0.134	0.130	0.125	0.119
25	0.135	0.135	0.135	0.136	0.137	0.137	0.138	0.138	0.139	0.139	0.139	0.139	0.139	0.138	0.137	0.134	0.130	0.125	0.118
30	0.135	0.135	0.136	0.136	0.137	0.138	0.138	0.139	0.139	0.140	0.140	0.140	0.140	0.139	0.137	0.135	0.131	0.125	0.117
35	0.136	0.136	0.136	0.137	0.137	0.138	0.139	0.139	0.140	0.140	0.140	0.141	0.140	0.140	0.138	0.135	0.130	0.124	
40	0.136	0.136	0.137	0.137	0.138	0.139	0.139	0.140	0.140	0.141	0.141	0.141	0.141	0.140	0.139	0.136	0.131		
45	0.136	0.136	0.137	0.138	0.138	0.139	0.140	0.140	0.141	0.141	0.142	0.142	0.142	0.141	0.140	0.136			
50	0.136	0.136	0.137	0.138	0.138	0.139	0.140	0.140	0.141	0.142	0.142	0.143	0.143	0.142	0.141				
55	0.136	0.136	0.137	0.138	0.138	0.139	0.140	0.141	0.141	0.142	0.143	0.143	0.144	0.144					
60	0.135	0.136	0.137	0.137	0.138	0.139	0.140	0.140	0.141	0.142	0.143	0.144	0.145						
65	0.134	0.135	0.136	0.137	0.138	0.138	0.139	0.140	0.140	0.141	0.142	0.144							
70	0.133	0.133	0.134	0.135	0.136	0.137	0.137	0.138	0.139	0.140	0.141								
75	0.130	0.131	0.132	0.133	0.134	0.134	0.135	0.135	0.136	0.136									
80	0.127	0.128	0.129	0.130	0.130	0.130	0.131	0.130	0.131										
85	0.122	0.123	0.124	0.125	0.125	0.125	0.125	0.124											
90	0.116	0.117	0.118	0.119	0.119	0.118	0.117												

Table 9.—$F_i(\alpha,\theta_1,\theta_2)$ for $\alpha = 35$.

35	0	5	10	15	20	25	30	35	40	45	50	55	60	65	70	75	80	85	90
0	0.130	0.131	0.131	0.132	0.132	0.132	0.133	0.133	0.133	0.133	0.133	0.132	0.131	0.129	0.127	0.123	0.118	0.113	0.108
5	0.131	0.131	0.131	0.132	0.132	0.133	0.133	0.133	0.134	0.134	0.133	0.133	0.132	0.130	0.127	0.124	0.120	0.115	0.111
10	0.131	0.131	0.132	0.132	0.133	0.133	0.134	0.134	0.134	0.134	0.134	0.134	0.133	0.131	0.129	0.126	0.121	0.117	0.113
15	0.132	0.132	0.132	0.133	0.133	0.134	0.134	0.135	0.135	0.135	0.135	0.135	0.134	0.132	0.130	0.127	0.123	0.118	0.114
20	0.132	0.132	0.133	0.133	0.134	0.135	0.135	0.136	0.136	0.136	0.136	0.136	0.135	0.134	0.131	0.128	0.123	0.118	0.113
25	0.132	0.133	0.133	0.134	0.135	0.135	0.136	0.136	0.137	0.137	0.137	0.137	0.136	0.135	0.132	0.128	0.123	0.118	
30	0.133	0.133	0.134	0.134	0.135	0.136	0.137	0.137	0.138	0.138	0.138	0.138	0.137	0.136	0.133	0.129	0.123		
35	0.133	0.133	0.134	0.135	0.136	0.136	0.137	0.138	0.138	0.139	0.139	0.139	0.138	0.136	0.134	0.129			
40	0.133	0.134	0.134	0.135	0.136	0.137	0.138	0.138	0.139	0.139	0.140	0.140	0.139	0.138	0.135				
45	0.133	0.134	0.134	0.135	0.136	0.137	0.138	0.139	0.139	0.140	0.141	0.141	0.140	0.139					
50	0.133	0.133	0.134	0.135	0.136	0.137	0.138	0.139	0.140	0.141	0.141	0.142	0.141						
55	0.132	0.133	0.134	0.135	0.136	0.137	0.138	0.139	0.140	0.141	0.142	0.142							
60	0.131	0.132	0.133	0.134	0.135	0.136	0.137	0.138	0.139	0.140	0.141								
65	0.129	0.130	0.131	0.132	0.134	0.135	0.136	0.136	0.138	0.139									
70	0.127	0.127	0.129	0.130	0.131	0.132	0.133	0.134	0.135										
75	0.123	0.124	0.126	0.127	0.128	0.128	0.129	0.129											
80	0.118	0.120	0.121	0.123	0.123	0.123	0.123												
85	0.113	0.115	0.117	0.118	0.118	0.118													
90	0.108	0.111	0.113	0.114	0.113														

Table 10.—$F_i(\alpha,\theta_1,\theta_2)$ for $\alpha = 40$.

40	0	5	10	15	20	25	30	35	40	45	50	55	60	65	70	75	80	85	90
0	0.129	0.129	0.129	0.130	0.131	0.131	0.131	0.132	0.131	0.131	0.130	0.129	0.127	0.124	0.121	0.117	0.113	0.111	0.112
5	0.129	0.129	0.130	0.130	0.131	0.131	0.132	0.132	0.132	0.132	0.131	0.130	0.128	0.126	0.122	0.119	0.115	0.114	0.119
10	0.129	0.130	0.130	0.131	0.132	0.132	0.133	0.133	0.133	0.133	0.132	0.131	0.130	0.127	0.124	0.121	0.118	0.118	0.123
15	0.130	0.130	0.131	0.132	0.132	0.133	0.134	0.134	0.134	0.134	0.134	0.133	0.131	0.129	0.126	0.123	0.120	0.119	
20	0.131	0.131	0.132	0.132	0.133	0.134	0.134	0.135	0.135	0.135	0.135	0.134	0.133	0.130	0.127	0.124	0.120		
25	0.131	0.131	0.132	0.133	0.134	0.135	0.135	0.136	0.136	0.136	0.136	0.135	0.134	0.132	0.128	0.124			
30	0.131	0.132	0.133	0.134	0.134	0.135	0.136	0.137	0.137	0.137	0.137	0.137	0.135	0.133	0.129				
35	0.132	0.132	0.133	0.134	0.135	0.136	0.137	0.137	0.138	0.138	0.138	0.138	0.136	0.134					
40	0.131	0.132	0.133	0.134	0.135	0.136	0.137	0.138	0.139	0.139	0.139	0.139	0.138						
45	0.131	0.132	0.133	0.134	0.135	0.136	0.137	0.138	0.139	0.140	0.140	0.140							
50	0.130	0.131	0.132	0.134	0.135	0.136	0.137	0.138	0.139	0.140	0.141								
55	0.129	0.130	0.131	0.133	0.134	0.135	0.137	0.138	0.139	0.140									
60	0.127	0.128	0.130	0.131	0.133	0.134	0.135	0.136	0.138										
65	0.124	0.126	0.127	0.129	0.130	0.132	0.133	0.134											
70	0.121	0.122	0.124	0.126	0.127	0.128	0.129												
75	0.117	0.119	0.121	0.123	0.124	0.124													
80	0.113	0.115	0.118	0.120	0.120														
85	0.111	0.114	0.118	0.119															
90	0.112	0.119	0.123																

Table 11.—$F_i(\alpha,\theta_1,\theta_2)$ for $\alpha = 45$.

45	0	5	10	15	20	25	30	35	40	45	50	55	60	65	70	75	80	85	90
0	0.128	0.128	0.129	0.129	0.130	0.130	0.131	0.131	0.130	0.130	0.128	0.126	0.124	0.121	0.117	0.115	0.116	0.124	0.166
5	0.128	0.128	0.129	0.130	0.130	0.131	0.131	0.131	0.131	0.130	0.129	0.127	0.125	0.123	0.120	0.119	0.123	0.140	
10	0.129	0.129	0.130	0.131	0.131	0.132	0.132	0.132	0.132	0.132	0.131	0.130	0.128	0.125	0.123	0.123	0.129		
15	0.129	0.130	0.131	0.131	0.132	0.133	0.133	0.134	0.134	0.134	0.133	0.132	0.130	0.127	0.126	0.125			
20	0.130	0.130	0.131	0.132	0.133	0.134	0.135	0.135	0.135	0.135	0.134	0.133	0.131	0.129	0.127				
25	0.130	0.131	0.132	0.133	0.134	0.135	0.136	0.136	0.136	0.136	0.136	0.135	0.133	0.130					
30	0.131	0.131	0.132	0.133	0.135	0.136	0.136	0.137	0.137	0.138	0.137	0.136	0.134						
35	0.131	0.131	0.132	0.134	0.135	0.136	0.137	0.138	0.138	0.139	0.138	0.137							
40	0.130	0.131	0.132	0.134	0.135	0.136	0.137	0.138	0.139	0.140	0.140								
45	0.130	0.130	0.132	0.134	0.135	0.136	0.138	0.139	0.140	0.141									
50	0.128	0.129	0.131	0.133	0.134	0.136	0.137	0.138	0.140										
55	0.126	0.127	0.130	0.132	0.133	0.135	0.136	0.137											
60	0.124	0.125	0.128	0.130	0.131	0.133	0.134												
65	0.121	0.123	0.125	0.127	0.129	0.130													
70	0.117	0.120	0.123	0.126	0.127														
75	0.115	0.119	0.123	0.125															
80	0.116	0.123	0.129																
85	0.124	0.140																	
90	0.166																		

Table 12.—$F_i(\alpha,\theta_1,\theta_2)$ for $\alpha = 50$.

50	0	5	10	15	20	25	30	35	40	45	50	55	60	65	70	75	80
0	0.127	0.128	0.129	0.129	0.130	0.131	0.131	0.130	0.130	0.128	0.127	0.124	0.122	0.120	0.120	0.126	0.166
5	0.128	0.128	0.129	0.130	0.131	0.131	0.131	0.131	0.131	0.130	0.128	0.126	0.125	0.124	0.128	0.143	
10	0.129	0.129	0.130	0.131	0.132	0.132	0.133	0.133	0.133	0.132	0.131	0.129	0.128	0.129	0.133		
15	0.129	0.130	0.131	0.132	0.133	0.134	0.134	0.135	0.135	0.134	0.133	0.132	0.131	0.131			
20	0.130	0.131	0.132	0.133	0.134	0.135	0.136	0.136	0.136	0.136	0.135	0.134	0.132				
25	0.131	0.131	0.132	0.134	0.135	0.136	0.137	0.138	0.138	0.137	0.137	0.135					
30	0.131	0.131	0.133	0.134	0.136	0.137	0.138	0.139	0.139	0.139	0.138						
35	0.130	0.131	0.133	0.135	0.136	0.138	0.139	0.140	0.140	0.140							
40	0.130	0.131	0.133	0.135	0.136	0.138	0.139	0.140	0.141								
45	0.128	0.130	0.132	0.134	0.136	0.137	0.139	0.140									
50	0.127	0.128	0.131	0.133	0.135	0.137	0.138										
55	0.124	0.126	0.129	0.132	0.134	0.135											
60	0.122	0.125	0.128	0.131	0.132												
65	0.120	0.124	0.129	0.131													
70	0.120	0.128	0.133														
75	0.126	0.143															
80	0.166																

Table 13.—$F_i(\alpha,\theta_1,\theta_2)$ for $\alpha = 55$.

55	0	5	10	15	20	25	30	35	40	45	50	55	60	65	70
0	0.128	0.128	0.129	0.130	0.131	0.131	0.131	0.131	0.129	0.128	0.126	0.124	0.124	0.129	0.166
5	0.128	0.129	0.130	0.131	0.132	0.132	0.132	0.132	0.131	0.130	0.129	0.129	0.132	0.146	
10	0.129	0.130	0.131	0.133	0.133	0.134	0.134	0.134	0.134	0.133	0.133	0.134	0.138		
15	0.130	0.131	0.133	0.134	0.135	0.136	0.136	0.137	0.136	0.136	0.136	0.136			
20	0.131	0.132	0.133	0.135	0.136	0.137	0.138	0.139	0.139	0.138	0.138				
25	0.131	0.132	0.134	0.136	0.137	0.139	0.140	0.140	0.140	0.140					
30	0.131	0.132	0.134	0.136	0.138	0.140	0.141	0.141	0.142						
35	0.131	0.132	0.134	0.137	0.139	0.140	0.141	0.142							
40	0.129	0.131	0.134	0.136	0.139	0.140	0.142								
45	0.128	0.130	0.133	0.136	0.138	0.140									
50	0.126	0.129	0.133	0.136	0.138										
55	0.124	0.129	0.134	0.136											
60	0.124	0.132	0.138												
65	0.129	0.146													
70	0.166														

Table 14.—$F_i(\alpha,\theta_1,\theta_2)$ for α = 60.

60	0	5	10	15	20	25	30	35	40	45	50	55	60
0	0.129	0.130	0.131	0.132	0.133	0.133	0.132	0.131	0.130	0.128	0.128	0.131	0.166
5	0.130	0.131	0.132	0.133	0.134	0.134	0.134	0.134	0.133	0.133	0.136	0.149	
10	0.131	0.132	0.134	0.135	0.136	0.137	0.137	0.137	0.137	0.138	0.142		
15	0.132	0.133	0.135	0.137	0.138	0.139	0.140	0.140	0.140	0.141			
20	0.133	0.134	0.136	0.138	0.140	0.141	0.142	0.142	0.143				
25	0.133	0.134	0.137	0.139	0.141	0.142	0.143	0.144					
30	0.132	0.134	0.137	0.140	0.142	0.143	0.145						
35	0.131	0.134	0.137	0.140	0.142	0.144							
40	0.130	0.133	0.137	0.140	0.143								
45	0.128	0.133	0.138	0.141									
50	0.128	0.136	0.142										
55	0.131	0.149											
60	0.166												

Table 15.—$F_i(\alpha,\theta_1,\theta_2)$ for α = 65.

65	0	5	10	15	20	25	30	35	40	45	50
0	0.131	0.132	0.134	0.135	0.135	0.135	0.134	0.132	0.132	0.134	0.166
5	0.132	0.133	0.135	0.136	0.137	0.137	0.137	0.138	0.140	0.152	
10	0.134	0.135	0.137	0.139	0.140	0.141	0.142	0.143	0.147		
15	0.135	0.136	0.139	0.141	0.143	0.144	0.145	0.146			
20	0.135	0.137	0.140	0.143	0.145	0.146	0.147				
25	0.135	0.137	0.141	0.144	0.146	0.148					
30	0.134	0.137	0.142	0.145	0.147						
35	0.132	0.138	0.143	0.146							
40	0.132	0.140	0.147								
45	0.134	0.152									
50	0.166										

Table 16.—$F_i(\alpha,\theta_1,\theta_2)$ for α = 70.

70	0	5	10	15	20	25	30	35	40
0	0.133	0.135	0.137	0.138	0.138	0.137	0.136	0.136	0.166
5	0.135	0.137	0.139	0.141	0.142	0.142	0.145	0.155	
10	0.137	0.139	0.142	0.145	0.146	0.148	0.151		
15	0.138	0.141	0.145	0.147	0.149	0.151			
20	0.138	0.142	0.146	0.149	0.152				
25	0.137	0.142	0.148	0.151					
30	0.136	0.145	0.151						
35	0.136	0.155							
40	0.166								

Table 17.—$F_i(\alpha,\theta_1,\theta_2)$ for α = 75.

75	0	5	10	15	20	25	30
0	0.136	0.138	0.141	0.141	0.140	0.139	0.166
5	0.138	0.142	0.145	0.147	0.149	0.158	
10	0.141	0.145	0.149	0.153	0.156		
15	0.141	0.147	0.153	0.156			
20	0.140	0.149	0.156				
25	0.139	0.158					
30	0.166						

Table 18.—$F_i(\alpha,\theta_1,\theta_2)$ for α = 80.

80	0	5	10	15	20
0	0.139	0.143	0.145	0.143	0.166
5	0.143	0.149	0.154	0.161	
10	0.145	0.154	0.161		
15	0.143	0.161			
20	0.166				

Table 19.—$F_i(\alpha,\theta_1,\theta_2)$ for α = 85.

85	0	5	10
0	0.142	0.148	0.166
5	0.148	0.165	
10	0.166		

Table 20.—$F_i(\alpha,\theta_1,\theta_2)$ for α = 90.

90	0
0	0.167

REPORT DOCUMENTATION PAGE

Form Approved
OMB No. 0704-0188

1. AGENCY USE ONLY (*Leave blank*)	2. REPORT DATE	3. REPORT TYPE AND DATES COVERED
	June 2005	Final Contractor Report

4. TITLE AND SUBTITLE

Capillary Driven Flows Along Differentially Wetted Interior Corners

5. FUNDING NUMBERS

WBS–22–101–53–01
NAG3–2741

6. AUTHOR(S)

C.L. Nardin and M.M. Weislogel

7. PERFORMING ORGANIZATION NAME(S) AND ADDRESS(ES)

Portland State University
P.O. Box 751
Portland, Oregon 97207–0751

8. PERFORMING ORGANIZATION REPORT NUMBER

E–15157

9. SPONSORING/MONITORING AGENCY NAME(S) AND ADDRESS(ES)

National Aeronautics and Space Administration
Washington, DC 20546–0001

10. SPONSORING/MONITORING AGENCY REPORT NUMBER

NASA CR—2005-213799

11. SUPPLEMENTARY NOTES

Project Manager, Eric L. Golliher, Microgravity Division, NASA Glenn Research Center, organization code RUF, 216–433–6575.

12a. DISTRIBUTION/AVAILABILITY STATEMENT

Unclassified - Unlimited
Subject Category: 34

Available electronically at http://gltrs.grc.nasa.gov

This publication is available from the NASA Center for AeroSpace Information, 301–621–0390.

12b. DISTRIBUTION CODE

13. ABSTRACT *(Maximum 200 words)*

Closed-form analytic solutions useful for the design of capillary flows in a variety of containers possessing interior corners were recently collected and reviewed. Low-g drop tower and aircraft experiments performed at NASA to date show excellent agreement between theory and experiment for perfectly wetting fluids. The analytical expressions are general in terms of contact angle, but do not account for variations in contact angle between the various surfaces within the system. Such conditions may be desirable for capillary containment or to compute the behavior of capillary corner flows in containers consisting of different materials with widely varying wetting characteristics. A simple coordinate rotation is employed to recast the governing system of equations for flows in containers with interior corners with differing contact angles on the faces of the corner. The result is that a large number of capillary driven corner flows may be predicted with only slightly modified geometric functions dependent on corner angle and the two (or more) contact angles of the system. A numerical solution is employed to verify the new problem formulation. The benchmarked computations support the use of the existing theoretical approach to geometries with variable wettability. Simple experiments to confirm the theoretical findings are recommended. Favorable agreement between such experiments and the present theory may argue well for the extension of the analytic results to predict fluid performance in future large length scale capillary fluid systems for spacecraft as well as for small scale capillary systems on Earth.

14. SUBJECT TERMS	15. NUMBER OF PAGES
Fluid dynamics	30
	16. PRICE CODE

17. SECURITY CLASSIFICATION OF REPORT	18. SECURITY CLASSIFICATION OF THIS PAGE	19. SECURITY CLASSIFICATION OF ABSTRACT	20. LIMITATION OF ABSTRACT
Unclassified	Unclassified	Unclassified	